

H II Region Abundances in the Polar Ring of NGC 2685¹

Paul B. Eskridge²

Department of Physics and Astronomy,
University of Alabama, Tuscaloosa, AL 35487

and

Richard W. Pogge³

Department of Astronomy,
The Ohio State University, Columbus OH 43210

ABSTRACT

We have obtained optical spectrophotometry of 11 H II regions in the polar ring of NGC 2685 (the Helix galaxy), and have used these data to study the physical characteristics of the polar-ring H II regions. The H II regions have normal spectra with no suggestion of unusual density, temperature, extinction, or composition. Semi-empirical calculations yield high oxygen abundance estimates (0.8–1.1 Z_{\odot}) in all H II regions. This, along with the observed ($B - V$) color, H α equivalent width, and molecular gas properties argue against the current picture in which polar rings form from tidally captured dwarf irregular galaxies, and suggests instead that the rings are long-lived, self-gravitating structures as predicted by some dynamical models. This would allow the time required for multiple generations of star formation, and for the retention of the resulting enriched ejecta for inclusion in further generations of star formation.

Subject headings: galaxies: abundances — galaxies: individual (NGC 2685) — galaxies: interactions — ISM: H II regions

¹This paper is partially based on observations obtained with the Multiple Mirror Telescope, a joint facility of the Smithsonian Institution and the University of Arizona.

²paul@hera.astr.ua.edu

³pogge@payne.mps.ohio-state.edu

1. Introduction

Polar-ring galaxies (PRGs) are unusual objects, typically composed of an early-type (E or S0) host galaxy, with a ring of material (stars, gas, and dust) orbiting in a plane roughly perpendicular to the major axis of the host galaxy. As such, they are clear examples of galaxy interactions and tidal accretion events. The first major study of the class of PRGs was that of Whitmore et al. (1990). This paper presented data on ~ 100 objects, only 6 of which were kinematically confirmed PRGs. Subsequent work has expanded this to a total of eleven objects (Combes et al. 1992; Arnaboldi et al. 1993; Reshetnikov & Combes 1994; Cox et al. 1995; Hagen-Thorn & Reshetnikov 1996). Whitmore et al. (1990) provides a good general overview of the properties of PRGs. The host galaxies are typically gas-poor systems, while the rings are gas-rich (Richter, Sackett & Sparke 1994), blue (Reshetnikov & Combes 1994), and dusty (Schweizer, Whitmore & Rubin 1983). PRGs also tend to be much more luminous in the far infrared (FIR) than typical early-type galaxies (Richter et al. 1994). Based on the H I masses, and optical colors of polar rings, the typical model for the ring donor is a tidally accreted dwarf irregular (dI) galaxy. Other possible donors are the outer parts of spiral galaxies, and primordial H I gas clouds.

There are three models that have been suggested to explain the apparent stability of polar rings. The first of these is due to Schweizer et al. (1983), who argue that polar rings are *not* stable, but can have very long decay times. They conclude that the timescale for the differential precession of the ring is on the order of a Hubble time for orbits sufficiently near the pole, but very short for orbits inclined by less than $\sim 70^\circ$. The second model, discussed by a number of groups (e.g. Dubinski & Christoudoulou 1994; Arnaboldi & Sparke 1994; Sackett & Sparke 1990), is that the rings are massive, self-gravitating structures that create stable polar orbits for themselves by deforming the potential of the host. The third model is that polar rings form in natural ‘islands of stability’: Polar orbits may be inherently stable if the host potential is oblate-triaxial, as suggested by Katz & Rix (1992) and Steiman-Cameron & Durisen (1988).

A great deal of recent work on PRGs has focussed on their use as probes of the extent and shape of the dark matter halos of their host galaxies. These studies interpret the kinematics of PRGs in terms of dynamical models, and thus assume PRGs to be at least quasi-equilibrium systems. On the whole, this work indicates PRGs to have very large mass-to-light ratios (e.g. Reshetnikov & Combes 1994), and substantially flattened dark matter halos (e.g. Sackett et al. 1994 and references therein). In a recent paper, Combes & Arnaboldi (1996) argue that the kinematic data for NGC 4650A can be fit by a model in which the dark matter is distributed following the polar-ring isophotes (and *not* the host galaxy). This is, in a sense, the extreme case of a self-gravitating model.

The fundamental questions regarding polar rings are as follows: How do the rings form? Once formed, how long do they last? One way of addressing these questions is to obtain abundance information on polar rings. All plausible candidates for the ring donors are low-abundance objects ($\lesssim 0.3$ Solar). For the rings to have high abundances would indicate that either our notions of ring formation are wrong, or that polar rings are long-lived, stable, self-gravitating structures. They must not only survive long enough to undergo the star-formation episodes required for self-enrichment, they must also be massive enough to retain their enriched ejecta. As polar rings typically have numerous H II regions, the easiest method to directly probe their abundances is nebular spectrophotometry of those H II regions. We have obtained such data for the prototype PRG NGC 2685, and we report our results in this paper. In §2 we provide background on NGC 2685. In §3 we describe our data set and reduction techniques. Our abundance analysis is presented in §4. We discuss our results for NGC 2685, and the possible implications for PRGs as a class in §5, and present a summary, along with our plans for continuing this project in §6.

2. Background on NGC 2685

NGC 2685 (Arp 336, also known as “The Helix galaxy” and “The Spindle”) has long been known to be an unusual galaxy (Sandage 1961). It is one of the two nearest PRGs (the other being NGC 660), and is thus one of the easiest to study in detail. NGC 2685 is a double ring system, with both an inner, polar ring, and an outer ring that is co-planar with the host-galaxy disk (see the images in Sandage 1961). Unless otherwise stated, when we refer to “the ring” we will be speaking of the polar ring. Some basic properties of the system are given in Table 1. The host galaxy and the ring are both fairly red. The system has $M_{HI}/L_B \approx 0.3$, similar to field dI galaxies (e.g. Roberts & Haynes 1994). The H I distribution was mapped by Shane (1980). His Westerbork data have a final resolution of $\sim 50''$, and show the H I to be associated with the inner and outer rings, with no detected emission from the host galaxy. A comparison with the single-dish observations of Richter et al. (1994) shows that the Westerbork maps are not missing any significant flux from extended emission. Hodge (1974) was the first to point out that the ring has a large population of H II regions. It is unclear if the CO $J = 1 - 0$ emission detected by Taniguchi et al. (1990) is coming from the ring, or from the host nucleus, however Watson, Guptill & Buchholz (1994) clearly detect CO $J = 2 - 1$ emission from the polar ring, and conclude that the ring is rich in molecular gas. NGC 2685 has no close, massive companions. There are two cataloged dIs within $\sim 30'$ (UGC 4683 and MCG+10-13-030). UGC 4683 has a comparable radial velocity to NGC 2685 ($V_{\odot} = 920$ km s $^{-1}$, de Vaucouleurs et al. 1991, hereafter RC3). There is no published velocity for MCG+10-13-030. There is a loose

group of galaxies between $\approx 1^\circ 5$ and $2^\circ 2$ north of NGC 2685, but all these systems have substantially higher radial velocities (1288–1518 km s⁻¹ – RC3). Thus they do not appear to be physically associated with NGC 2685.

3. Data Acquisition and Reduction

We obtained optical spectrophotometry of eleven H II regions in the polar ring of NGC 2685 with the MMT Blue Channel Spectrograph on three successive nights in November and December 1994. Table 2 gives the details of the observations. The detector was a Loral 3072×1024 CCD. We used the 500g/mm $\lambda_B=5410\text{\AA}$ grating, and a $1'' \times 180''$ slit, resulting in a spectral range of 3500 \AA — 7100 \AA , and a spectral resolution of $\sim 5\text{\AA}$ (FWHM), with a sampling of 1.15 \AA per pixel. We binned the data by 2 pixels in the spatial direction before read-out, giving a spatial sampling of 0".6 per binned pixel. The seeing was $\sim 1''$ –1".5 throughout the run, and the weather was photometric. Figure 1 shows a continuum-subtracted H α + [N II] emission line image of NGC 2685 obtained with the Ohio State Imaging Fabry-Perot Spectrometer (Pogge et al. 1995) in direct imaging mode on the 1.8m Perkins telescope of the Ohio Wesleyan and Ohio State Universities in Flagstaff Arizona. We have marked the observed H II regions and the slit positions on this image.

In addition to the ring H II regions, Fig. 1 shows extended H α emission around the nucleus of NGC 2685. This emission was discovered by Ulrich (1975). The gas is rotating about the minor axis of the host, and has a LINER-type spectrum. The H α morphology of this material is asymmetric; the emission is much stronger to the NW than to the SE. This is also obvious from the [O II] $\lambda 3727\text{\AA}$ line-intensities shown by Ulrich (1975). Her spectra also show that the NW side is the approaching side. This, and our continuum imaging lead us to believe that the asymmetry is largely due to internal extinction in NGC 2685.

We corrected our data for bias, overscan, and flat-field patterns in the standard way, using VISTA (Stover 1988). We prepared the slit-illumination frame using IRAF⁴. We extracted 1-D spectra from the images using the spectrum of a bright continuum source as a trace of the positional variation along the dispersion axis. We obtained HeNeAr lamp frames before and after each target observation to provide the primary wavelength calibrations. Typically, we had to apply small secondary corrections from the night-sky lines on the actual data frames. We used 20–50 pixel regions near the ends of the slits

⁴IRAF is distributed by the National Optical Astronomy Observatories, which are operated by the Association of Universities for Research in Astronomy, under cooperative agreement with the National Science Foundation.

to determine the sky subtraction. We used the KPNO tables to correct the spectra for atmospheric extinction.

We obtained repeated observations of the spectrophotometric standards Feige 15, Feige 34, and Hiltner 600 throughout each night in order to flux calibrate our spectra. We observed the standards with a $5'' \times 180''$ slit to minimize slit-losses. We emphasize that although the absolute flux calibration of our spectra is subject to unknown systematics due to such things as slit placement, sky subtraction, slit losses, and tracking errors, the relative line fluxes should be accurately determined. As we obtained spectra at a number of position angles, often quite far from the parallactic angle, and over a moderate range in air-mass (typically 1.1–1.4), we investigated the possibility that our results are compromised by atmospheric dispersion. From a comparison of the relative line fluxes of $H\alpha$ and $[O\ II]$ in spectra of the H II region R2, obtained over a range of air-masses, we found no evidence of the sort of systematic changes in flux ratios that would indicate a substantial problem due to atmospheric dispersion.

After flux-calibrating the individual exposures, we measured the centroids of the bright emission lines, and used these data to correct all exposures of a given H II region to the same wavelength scale. The individual exposures were then merged, providing total exposure times of between 2 and 7 hours for each H II region. In Figure 2, we present the final spectra for two of our targets, demonstrating the full range in quality of our dataset.

4. Abundance Analysis

We extracted emission line fluxes and equivalent widths from our spectra using the VISTA package LINER (Pogge & Owen 1993). As we do not detect $[O\ III]\ \lambda 4363\text{\AA}$ in any of our spectra, we also evaluated the continuum rms at $\sim 4350\text{\AA}$, to determine upper limits for this line. The recessional velocity of NGC 2685 (see Table 1) puts the Hg I 4358 \AA emission line from the Tucson streetlights into the spectral region between $H\gamma$ and $[O\ III]\ 4363\text{\AA}$. We avoid this region in estimating the upper limit on $[O\ III]\ 4363\text{\AA}$ emission. We used the following procedure for our line-analysis:

The foreground absorption for NGC 2685 is $A_B = 0.16(\text{RC3})$. We found that our results were generally more self-consistent if we did not correct for this explicitly, but instead determined an overall estimate for the absorption using the Balmer decrement. This is a reasonable approach due to the small redshift of NGC 2685. The calculation was complicated by the aforementioned Hg I 4358 \AA contamination which prevented us from measuring $H\gamma$ in our spectra. However most of our spectra have good detections of $H\delta$,

giving us at least two Balmer line ratios with which to determine the Balmer decrement. We note that most of our sample have *total* computed A_V 's that are less than the *foreground* value of 0.12 mag (for $R_V = 3.1$) from the RC3.

We used the observed fluxes of the [O III] $\lambda 4959\text{\AA}$, and [O III] $\lambda 5007\text{\AA}$ lines, along with the 3σ upper limits to the [O III] $\lambda 4363\text{\AA}$ line to determine upper limits to T_e following the prescriptions in Osterbrock (1989), and assuming the electron density (N_e) in the low-density limit. We then used the flux ratio of the [S II] $\lambda\lambda 6717, 6731\text{\AA}$ lines to determine N_e for a range of temperatures consistent with the T_e limits. This was accomplished following Osterbrock (1989), but using the updated atomic physics calculations of Cai & Pradhan (1993). We note that the derived densities are commensurate with our assumption of the low-density limit in our T_e calculations in all cases.

We determined total A_V estimates from the ratios of the Balmer lines, using Case B recombination, (Osterbrock 1989) for $T_e = 10^4$ K, and assuming absorption equivalent widths of 2\AA for the Balmer sequence (following McCall, Rybski & Shields 1985). For a derived $A_V < 0.05$ no extinction correction was made. For $A_V \geq 0.05$, we used the extinction curve of Cardelli, Clayton & Mathis (1989). In Table 3 we present the line strengths for all detected lines in all our targets. The line strengths are scaled to the $H\beta$ fluxes. We give the measured fluxes before correction for extinction and Balmer absorption (f/f_β), and after these corrections (I/I_β). We also give the measured equivalent widths in \AA , and the statistical signal to noise for each line.

As we do not detect [O III] $\lambda 4363\text{\AA}$ in any of our H II region spectra, we cannot derive the oxygen abundance directly. Instead we use the semi-empirical R_{23} method (e.g. Edmunds & Pagel 1984; Dopita & Evans 1986) to determine the oxygen abundances. R_{23} is defined as follows:

$$R_{23} = \frac{f_{3727} + f_{4959} + f_{5007}}{f_{H\beta}}, \quad (1)$$

where the f 's represent the fully corrected fluxes for the given lines. As the R_{23} -oxygen abundance relationship is double-valued, we need to determine which branch of the R_{23} -abundance curve is appropriate for our objects. Typically, this is done using the ratio of [N II] $\lambda 6583\text{\AA}$ to [O II] $\lambda 3727\text{\AA}$ (McGaugh 1994, Ryder 1995), where $\log([\text{N II}]/[\text{O II}]) > -1$ implies use of the high-abundance branch. This criterion hold for all our sample. We thus adopt the upper abundance branch calibration of R_{23} with $12 + \log(O/H)$ of Dopita & Evans (1986), as presented by Oey & Kennicutt (1993). We present these results, with all other derived quantities for our sample, in Table 4.

The derived O/H abundances listed in Table 4 are limited by a systematic uncertainty of ~ 0.2 dex in $12 + \log(O/H)$ in the absolute calibration of R_{23} (Oey & Kennicutt 1993).

By comparison, the formal statistical uncertainties in the derived $12 + \log(O/H)$ based on measurement errors in R_{23} range from ~ 0.13 dex for H II regions with the lowest signal-to-noise spectra (R8b and R9), to $\lesssim 0.05$ dex in the best spectra.

5. Discussion

The oxygen abundances we derive for the 11 H II regions in our sample are in the range $8.82 \leq 12 + \log(O/H) \leq 8.98$, with an average value of $12 + \log(O/H) \approx 8.92$ for the polar ring. Taking $12 + \log(O/H)_{\odot} = 8.93$ (Grevesse & Anders 1989), this means the H II regions in our sample have oxygen abundances of 0.8–1.1 Z_{\odot} . We compare this with the results of Zaritsky, Kennicutt & Huchra (1994), who obtained similar data for a sample of field spirals. Our abundance result matches the median of their Sc sample, and fits in the range of their Sbc’s. When combined with other observed properties, as discussed below, this poses a substantial problem for understanding the origin and chemical enrichment history of the polar ring in NGC 2685.

As discussed in §1, polar rings are typically considered to be debris of captured dI galaxies. Such systems are metal-poor in all studied cases (e.g. Mathews, Boyd & Fuller 1993). Other possible sources of the ring material (the outer part of a spiral, or primordial H I gas) will also be metal-poor. In fact, there are few, if any, easily accretable sources of high-abundance gas in the Universe. Further, NGC 2685 is *not* a particularly luminous system (see Table 1). It has a total V -band luminosity roughly that of M33 (van den Bergh 1992). It is therefore very difficult to imagine that it could have accreted metal-rich gas from deep in the potential well of a more massive spiral disk. Thus, for the gas to be metal-rich, it must have self-enriched, despite the fact that dIs of similar overall properties (gas-content and luminosity) have not been able to do so. This means that the polar ring surrounding NGC 2685 must be both stable (with a lifetime comparable to the Hubble time) *and* self-gravitating.

We have observed only one H II region from the outer ring (R9). While our spectrum of this object has the lowest signal to noise in our dataset, it appears to have an oxygen abundance similar to those found for the inner ring H II regions. We thus see no evidence for significantly different abundances in the two rings. We also see no evidence for any azimuthal pattern in our abundance results. This argues that the ring gas is likely to be dynamically well-mixed, and that our results indicate a generally high oxygen abundance in the ring gas, rather than local enrichment.

Our results thus strongly support the self-gravitating model of PRGs in the case of

NGC 2685. This is curious, due to the complex appearance of the system. NGC 2685 possesses both an inner (polar) ring, and an outer (planar) ring. Further, the appearance of the inner ring is anything but smooth and relaxed (NGC 2685 has long been known as “The Helix Galaxy” and “The Spindle” after all). These results thus pose the following problem for dynamical modellers: Is it possible to construct a stable, self-consistent model of a self-gravitating ring structure that reproduces the apparent complexity of NGC 2685? The work of Steiman-Cameron, Kormendy & Durisen (1992) indicates that it may be, but certainly the question is far from resolved. The most detailed work on dynamical modelling of NGC 2685 is that of Peletier & Christodoulou (1993), who modelled the two-ring structure, but did not attempt to reproduce the complex appearance of the inner ring. They concluded that a double-ring structure such as that of NGC 2685 can be very long lived if the underlying potential is triaxial. They also argue that the ring stars have a mean age of no more than 5–6 Gyr, based on the broad-band colors of the ring, and an assumption that the ring is fairly metal-poor. Our results argue against this assumption, and thus indicate a substantially younger photometric age for the (optical) mean stellar population.

We now turn our attention to fitting together the implications of the observed photometric, chemical, and dynamical properties of the polar ring. As noted in §2, the H I distribution in NGC 2685 was mapped by Shane (1980). Although recent high resolution aperture synthesis observations of the H I in NGC 4650A (Arnaboldi et al. 1997) reveal that earlier VLA (van Gorkom, Schechter & Kristian 1987) data had seriously underestimated the total H I content, we do not believe that this is a serious possibility in the case of NGC 2685. For NGC 4650A, the H I content from single-dish measurements (Richter et al. 1994) is substantially higher than that from the VLA data, and agrees reasonably well with the new ATCA data of Arnaboldi et al. (1997). No such disagreement exists between the single-dish and Westerbork results for NGC 2685. So, taking Shane’s (1980) results for the H I and dynamical mass of the polar ring, we find $(M_{HI}/M_{dyn})_{ring} \approx 0.15$. According to Roberts & Haynes (1994), this is typical of an Sm or Im system. However, Peletier & Christodoulou (1993) give a $(B - V) \approx 0.8$ for the polar ring. This is quite red; Roberts & Haynes (1994) find $(B - V) \approx 0.8$ typical of S0/a to Sa galaxies. Thus, although the polar ring has an H I content typical of an Im, it is substantially redder than such galaxies.

Peletier & Christodoulou (1993) note that their colors may be reddened by the dust in the polar ring. If the true color of the ring is assumed to be a typical Im value ($(B - V) \approx 0.4$), then one must assume $E(B - V) \approx 0.4$ from internal extinction. This is quite high, and requires a large (but very model dependent – e.g. Davies et al. 1993; Witt, Thronson & Capuano 1992) dust content, compared to that of a typical Im. Of course abundance is known to correlate with dust content in galaxies (e.g. van den Bergh & Pierce 1990). Thus our abundance results argue for a higher relative dust content than

might be found in a low abundance dI. In fact, while the polar ring is obviously dusty (see the image in Sandage 1961), the FIR properties of NGC 2685 do not suggest an unusually high dust content. Richter et al. (1994) find an *IRAS* FIR to blue luminosity ratio of $L_{FIR}/L_B \approx -0.53$, only slightly higher than the mean values of -0.62 and -0.88 ± 0.05 derived for samples of S0s by Thronson, Bally & Hacking (1989) and Eskridge & Pogge (1991). The L_{FIR}/L_B for the ring only will, of course, be higher. Eskridge & Pogge (1991) also note that NGC 2685 is H I rich for its FIR flux, compared to a sample of S0s. This may be largely due to the majority of the H I being associated with the outer ring. Thronson et al. (1989) derive a dust mass for NGC 2685 based on its *IRAS* flux. Scaled to our distance estimate, this is $M_d \approx 10^5 M_\odot$. If we assume that all the FIR originates from the polar ring (unlikely, as the host galaxy has a LINER nucleus), this means $M_{dust}/M_{HI} \approx 10^{-4}$. This argues against the existence of a vast quantity of dust in the polar ring. Finally, we note that NGC 2685 falls in the midst of the distribution of L_{FIR}/L_B for Im galaxies in the sample of Melisse & Israel (1994), but falls at the very low end of their distribution for Sc spirals. In summary, while the polar ring is clearly dusty, it is unlikely to have an internal extinction as high as $E(B - V) \approx 0.4$

We have measured a total $H\alpha + [N II]$ equivalent width of 12\AA for the polar ring from our $H\alpha$ imaging data. This is actually a lower limit, as there is clearly contamination in our continuum from the underlying host galaxy. We use our equivalent width, and the $(B - V)$ color of Peletier & Christodoulou to compare the polar ring of NGC 2685 to the spiral galaxy disk models of Kennicutt, Tamblyn & Congdon (1994). We find reasonably good matches for the observed $H\alpha$ equivalent width and $(B - V)$ color with two models. One has a birthrate parameter of $b \approx 0.14$ and exponentially decaying star formation with a decay timescale of $\tau \approx 3.2$ Gyr for a Kennicutt (1983) IMF. The other has $b \approx 0.09$ and $\tau \approx 2.6$ Gyr for a Salpeter (1955) IMF. The range of birthrate parameters we derive from the two good models overlap the Kennicutt et al. (1994) results for Sa and Sab galaxies. We cannot obtain a reasonable fit with the Scalo (1986) IMF; the model that comes closest is substantially too blue ($(B - V) \approx 0.58$). If we assume that such a model is correct (i.e. that the measured $(B - V)$ color is strongly effected by reddening), then the Scalo IMF model yields a very high birthrate parameter ($b \approx 0.7$), and an unconstrained decay time for star formation ($\tau \gtrsim 8$ Gyr). That is, a basically constant rate of star formation over the Hubble time.

Finally, we can use our abundance measurement and the ring gas content to examine the chemical enrichment history of the polar ring compared with typical spiral galaxies. It is well known that the simple closed-box model for chemical evolution (e.g. Schmidt 1963) overpredicts the enrichment for field spiral galaxies (e.g. Shields, Skillman & Kennicutt

1991). The closed-box formalism is expressed

$$Z = y \ln \mu^{-1}, \quad (2)$$

where Z is the overall or specific abundance in question, y is the yield per unit mass of star formation, and μ is the gas mass fraction. As noted above, the results of Shane (1980) give $(M_{HI}/M_{dyn})_{ring} \approx 0.15$, or $\ln \mu \approx -1.9$ in typical notation. Comparing this and our oxygen abundance to the field and Virgo cluster spiral samples of Shields et al. (1991), we find that the polar ring is substantially more enriched than field galaxies of a similar μ . The abundance is marginally below the simple closed-box model prediction, and substantially lower than that observed for Virgo cluster spirals of similar μ .

This comparison has been done ignoring molecular gas. The CO $J = 1 - 0$ observation of Taniguchi et al. (1990) was a single pointing, centered on the galaxy nucleus. It is unclear if the gas they detect is associated with the ring or the host galaxy. Watson et al. (1994) clearly detect CO $J = 2 - 1$ emission from a map made along the long axis of the polar ring. They detect the rotation of the ring in their data; the molecular gas is clearly associated with the polar ring. Watson et al. (1994) derive an estimate of $4.5 \pm 0.9 \times 10^8 M_{\odot}$ for the molecular mass of the polar ring (scaled to our assumed distance) assuming the $I_{CO}-M_{H_2}$ relationship of Young & Scoville (1991), and further assuming the ratio of CO $J = 2 - 1$ to CO $J = 1 - 0$ to be ~ 0.7 . It is clear that the $I_{CO}-M_{H_2}$ depends on abundance (e.g. Arimoto, Sofue & Tsujimoto 1996). However, the ring has essentially Solar abundance, and thus this should not be a factor. It has also been shown (e.g. Maloney & Black 1988) that the excitation temperature of the molecular gas (or equivalently, the density of the interstellar radiation field) also effects the $I_{CO}-M_{H_2}$ ratio. Thus a high excitation temperature of the molecular gas may be inflating the mass estimate of Watson et al. (1994).

We point this out for the following reason: Watson et al. (1994) derive an estimate of $\log(M_{H_2}/M_{HI}) \approx 0.65$. This is above Young & Scoville’s median value for S0-Sa galaxies, but well within the range. Young & Scoville find a few spirals as late as Sc with $\log(M_{H_2}/M_{HI})$ values as high as ~ 0.65 . This, despite an observed M_{HI}/M_{dyn} equal to that found for irregulars. Furthermore, if we accept the Watson et al. (1994) result, this gives $(M_{gas}/M_{dyn})_{ring} \approx 0.73$, or $\ln \mu \approx -0.3$. It seems implausible, at best, that a red, Solar abundance ring can have $\sim 75\%$ of its total *dynamical* mass in the form of gas. If we instead simply assume that the M_{H_2}/M_{HI} ratio is of order unity, we derive $\ln \mu \approx -1.2$. All systems (both in Virgo and the field) with such high μ values in the study of Shields et al. (1991) have substantially sub-Solar oxygen abundances. Our observed (\sim Solar) abundance is roughly half a dex higher than these systems, and falls exactly on the prediction from the simple closed box model.

We conclude by considering the implications of this work in the context of the recent

papers of Galletta, Sage & Sparke (1997) and Arnaboldi et al. (1997). As we mentioned above, Arnaboldi et al. (1997) present new ATCA H I observations of NGC 4650A, and conclude that the total H I content of the polar ring is nearly twice that indicated by earlier VLA data. The total H I mass of NGC 4650A is $\sim 8 \times 10^9 M_\odot$, comparable to a typical Sb spiral (Roberts & Haynes 1994). Arnaboldi et al. (1997) further conclude that the kinematics of the H I reveal evidence for spiral structure in the polar ring. NGC 2685 and NGC 4650A define the extremes of PRG morphology. In NGC 2685, the radius of the polar ring is small compared to the optical radius of the host galaxy, while in NGC 4650A, the ring extends out to several host optical radii. Thus while the systems cannot be simply compared, they both present enormous difficulties for models that attempt to form polar rings out of material that is easily accreted in the Universe today.

Galletta et al. (1997) present CO $J = 1 - 0$ observations for a sample 10 objects from the catalog of Whitmore et al. (1990). They supplement this with observations of two other systems (including NGC 2685) taken from the literature. They derive H_2 mass estimates for their sample from their CO $J = 1 - 0$ observations, assuming the Galactic calibration of Solomon et al. (1987). The Galletta et al. (1997) H_2 mass estimates are in the range $10^{8-9} M_\odot$, with M_{H_2}/M_{HI} typically 0.1 — 0.7. While the calibration of H_2 mass with CO line intensity is uncertain at best, the key point is that PRGs tend to be quite rich in molecular gas compared to dI systems. Indeed, they approach M_{H_2}/M_{HI} values typical of normal spiral galaxies (e.g. Sage 1993), although the overall H_2 masses are small compared to typical spirals.

The available data, and a number of dynamical models indicate the polar rings are stable, long-lived structures. Furthermore, this work, and others that we have cited above reveal the rings to have physical and chemical properties unlike those of any plausible gas donor that exists currently. We speculate that polar rings were formed early in the history of galaxy evolution by interactions with relative angular momenta that favored capture into inclined orbits, rather than full mergers. Thus the properties of such stable, old polar rings could provide us with information on the nature of the objects that merged to form normal galaxies in the current Universe.

6. Summary and Plans for Future Work

We have presented the results of our spectrophotometric study of H II regions in the polar ring of NGC 2685. The oxygen abundances of the 11 H II regions in our sample are all in the range 0.8—1.1 Z_\odot , with no evidence for any azimuthal abundance pattern. Thus the polar ring has a gas phase abundance typical of Sbc or Sc spirals, despite having an H I

content (and mass fraction) typical of a dI galaxy. At first glance this appears to require the polar ring to be a long-lived, self gravitating feature, despite its obvious complexity. While this may be the case, a more careful consideration of the observed properties of the ring make it clear that the ring cannot be the remnant of anything like a current dI galaxy. It has a $(B - V)$ color as red as a typical S0/a or Sa galaxy. This, combined with its $H\alpha$ equivalent width, indicates a starforming history typical of an Sa or Sab spiral. It has molecular gas properties that are more in keeping with an early-type disk galaxy than a dI. Finally, it is one of those rarest of objects that is actually well-fit by the simple closed-box chemical enrichment model.

What this seems to require is that the host galaxy accreted a low-luminosity object that was either already enriched at the time of the interaction, or that was massive enough (despite its low optical luminosity) to retain the enrichment products of stellar evolution over the course of the subsequent history of the system. There are no obvious field counterparts of either such object in the Universe today.

We cannot draw any sweeping conclusions regarding the class of polar-ring galaxies based on these results for one object. Rather, they indicate that a larger study is warranted. We have obtained the necessary spectrophotometry for two other kinematically confirmed PRGs, and have the $H\alpha$ imaging needed to define spectrophotometric targets for seven of the remaining eight currently confirmed PRGs.

We take great pleasure in thanking Carol Heller for being a superb MMT Operator, and the MMT TAC for awarding us the observing time. We also thank Bill Keel and Dimitris Christodoulou for helpful discussion, and the referee for several excellent suggestions. The OSU IFPS instrument project was supported by NSF Grants AST-8822009 and AST-9112879. This research was partially supported by the EPSCoR program under grant EHR-9108761.

REFERENCES

- Arimoto, N., Sofue, Y., & Tsujimoto, T. 1996, PASJ, 48, 275.
- Arnaboldi, M., Capaccioli, M., Cappellaro, E., Held, E.V., & Sparke, L., 1993, A&A, 267, 21.
- Arnaboldi, M., Oosterloo, T., Combes, F., Freeman, K.C., & Koribalski, B. 1997, AJ, 113, 585.
- Arnaboldi, M., & Sparke, L.S., 1994, AJ, 107, 598.

- Cai, W., & Pradhan, A.K. 1993, ApJS, 88, 329.
- Cardelli, J.A., Clayton, G.C., & Mathis, J.S. 1989, ApJ, 345, 245.
- Combes, F., & Arnaboldi, M., 1996, A&A, 305, 763.
- Combes, F., Braine, J., Casoli, F., Gerin, M., & van Driel, W., 1992 A&A, 259, L65.
- Cox, A.L., Sparke, L.S., Richter, O., & Shaw, M., 1995 in “Three-Dimensional Systems,” Annals of the NY Academy of Sciences v. 751, eds. H.E. Kandrump, S.T. Gottesman, & J.R. Ipser (NY Academy Press: New York) p. 27.
- Davies, J.I., Phillipps, S., Boyce, P.J., & Disney, M.J. 1993, MNRAS, 260, 491.
- de Vaucouleurs, G., de Vaucouleurs A., Corwin, H.G., Jr., Buta, R.J., Paturel, G., & Fouqué, P. 1991, Third Reference Catalogue of Bright Galaxies (Springer-Verlag: New York).
- Dopita, M.A., & Evans, I.N. 1986, ApJ, 307, 431.
- Dubinsky, J., & Christoudoulou, D.M., 1994, ApJ, 424, 615.
- Edmunds, M.G., & Pagel, B.E.J. 1984, MNRAS, 211, 507.
- Eskridge, P.B., & Pogge, R.W. 1991, AJ, 101, 2056.
- Galletta, G., Sage, L.J., & Sparke, L.S. 1997, MNRAS, 284, 773.
- Grevesse, N., & Anders, E. 1989 in “Cosmic Abundances of Matter,” AIP Conference Proceedings v. 183, (AIP Press: New York) p. 1.
- Hagen-Thorn, V.A., & Reshetnikov, V.P. 1996 ALet, 22, 677.
- Hodge, P.W. 1974 ApJS, 27 113.
- Katz, N., & Rix, H.-W., 1992, ApJ, 389, L55.
- Kennicutt, R.C., Jr. 1983, ApJ, 272, 54.
- Kennicutt, R.C., Jr., Tamblyn, P., & Congdon, C.W. 1994, ApJ, 435, 22.
- Maloney, P., & Black, J.H. 1988, ApJ, 325, 389.
- Mathews, G.J., Boyd, R.N., & Fuller, G.M., 1993, ApJ, 403, 65.
- McCall, M.L., Rybski, P.M., & Shields, G.A. 1985, ApJS, 57, 1.
- McGaugh, S.S. 1994, ApJ, 426, 135.
- Melisse, J.P.M., & Israel, F.P. 1994, A&A, 285, 51.
- Oey, M.S., & Kennicutt, R.C. 1993, ApJ, 411, 137.
- Osterbrock, D.E. 1989, Astrophysics of Gaseous Nebulae and Active Galactic Nuclei (University Science Books: Mill Valley).

- Peletier, R.F., & Christodoulou, D.M., 1993, *AJ*, 105, 1378.
- Pogge, R.W., & Owen, J.M. 1993, *LINER; An Interactive Spectral Line Analysis Program*, OSU Internal Report 93–01.
- Pogge, R.W., Atwood, B., Byard, P.L., O’Brien, T.P., Peterson, B.M., Lame, N.J., & Baldwin, J.A. 1995, *PASP*, 107, 1226.
- Reshetnikov, V.P., & Combes, F., 1994, *A&A*, 291, 57
- Richter, O.-G., Sackett, P.D., & Sparke, L.S., 1994, *AJ*, 107, 99.
- Roberts, M.S., & Haynes, M.P. 1994 *ARA&A*, 32, 115.
- Ryder, S.D. 1995, *ApJ*, 444, 610.
- Sackett, P.D., Rix, H.-W., Jarvis, B.J, & Freeman, K.C., 1994, *ApJ*, 436, 629.
- Sackett, P.D., & Sparke, L.S., 1990, *ApJ*, 361, 408.
- Sage, L.J. 1993, *A&A*, 272, 123.
- Salpeter, E.E. 1955, *ApJ*, 121, 161.
- Sandage, A. 1961, *The Hubble Atlas of Galaxies*. (Carnegie Institute of Washington: Washington DC).
- Scalo, 1986, *Fund. Cos. Phys.*, 11, 1.
- Schmidt, M. 1963, *ApJ*, 137, 758.
- Schweizer, F., Whitmore, B.C., & Rubin, V.C., 1983, *AJ*, 88, 909.
- Shane, W.W. 1980, *A&A*, 82, 314.
- Solomon, P.M., Rivolo, A.R., Barrett, J.W., & Yahil, A. 1987, *ApJ*, 319, 730.
- Steiman-Cameron, T.Y., & Durisen, R.H., 1988, *ApJ*, 325, 26.
- Steiman-Cameron, T.Y., Kormendy, J., & Durisen, R.H., 1992, *AJ*, 104, 1339.
- Shields, G.A., Skillman, E.D., & Kennicutt, R.C., Jr. 1991, *ApJ*, 371, 82.
- Stover, R.J., 1988, in “Instrumentation for Ground-based Optical Astronomy: Present and Future,” ed. L.B. Robinson (Springer: New York), p. 443.
- Taniguchi, Y., Sofue, Y., Wakamatsu, K.-I., & Nakai, N., 1990, *AJ*, 100, 1086.
- Thronson, H.A., Bally, J., & Hacking, P., 1989, *AJ*, 97, 363.
- Thronson, H.A., Jr., Tacconi, L., Kenney, J., Greenhouse, M.A., Margulis, M., Tacconi-Garman, L., & Young, J.S. 1989, *ApJ*, 344, 747.
- Ulrich, M.-H. 1975, *PASP*, 87, 965.

- van den Bergh, S., & Pierce, M.J., 1990, ApJ, 364, 444.
- van den Bergh, S., 1992, A&A, 264, 75.
- van Gorkom, J.H., Schechter, P.L., & Kristian, J. 1987, ApJ, 314, 457.
- Watson, D.M., Guptill, M.T., & Buchholz, L.M. 1994, ApJ, 420, L21.
- Whitmore, B.C., Lucas, R.A., McElroy, D.B., Steiman-Cameron, T.Y., Sackett, P.D., & Olling, R.P., 1990, AJ, 100, 1489.
- Witt, A.N., Thronson, H.A., Jr., & Capuano, J.M., Jr., 1992, ApJ, 393, 611.
- Yahil, A., Tammann, G.A., & Sandage, A. 1977, ApJ, 217, 903.
- Young, J.S., & Scoville, N.Z. 1991, ARA&A, 29, 581.
- Zaritsky, D., Kennicutt, R.C., Jr., & Huchra, J.P. 1994 ApJ, 420, 87.

Table 1 – Basic Properties

		References
$\alpha(1950.0)$	08 ^h 51 ^m 41 ^s .2	1
$\delta(1950.0)$	+58°55'30"	1
m_B	12.12	1
V_\odot	883 km s ⁻¹	1
D	13.4 Mpc	1,2
M_B	-18.5	1,2
$(B - V)_{host}$	~0.9	3
$(B - V)_{ring}$	~0.8	3
S_{HI}	34.2 ± 4.0 Jy km s ⁻¹	4
M_{HI}	~1.4 × 10 ⁹ M _⊙	4,2
M_{HI}/L_B	~0.3	4
log(FIR)	-13.50	4
L_{FIR}	~1.8 × 10 ⁹ L _⊙	4,2
$I_{CO}(1 \rightarrow 0)$	14.7 ± 1.2 K km s ⁻¹	5
$I_{CO}(2 \rightarrow 1)$	25.1 K km s ⁻¹	6

1) de Vaucouleurs et al. 1991. 2) Distance derived using the Yahil, Tammann & Sandage (1977) formalism, and $H_0 = 75$ km s⁻¹ Mpc⁻¹. 3) Peletier & Christodoulou (1993). 4) Richter et al. (1994). 5) Taniguchi et al. (1990). 6) Watson et al. (1994).

Table 2 – Observing Log

UT Date	Slit PA °	Slit Offsets "E, "N	H II Regions	Total Exposure sec
30 Nov. 1994	15	34, -16	R1,R4,R5	7200
	55	-30, 18	R2,R6,R8a,R8b	3600
01 Dec. 1994	55	-30, 18	R2,R6,R8a,R8b	3600
	16	-26, 0	R2,R3,R8c,R9	9000
02 Dec. 1994	90	0, 27	R2,R7	9000
	15	34, -16	R1,R4,R5	1800

Table 3 – Line Strengths

	R1	R2	R3	R4	R5	R6	R7	R8a	R8b	R8c	R9
[O II] $\lambda 3727$											
f/f_{β}^1	1.63	1.71	2.06	2.36	1.91	1.96	1.92	2.10	2.18	2.45	2.22
I/I_{β}^2	1.62	2.14	1.79	2.21	1.81	1.78	1.67	1.80	2.47	1.97	2.19
Eq. Width ³	81.30	141.2	56.66	53.50	41.04	40.06	54.47	36.38	60.78	42.15	20.51
σ^4	16.0	11.3	12.9	10.8	6.9	10.9	12.0	4.9	4.7	5.0	3.8
H ζ $\lambda 3889$											
	0.07	0.11									
	0.11	0.16									
	3.85	10.39									
	2.6	1.4									
H ϵ $\lambda 3969$											
	0.12	0.09									
	0.15	0.14									
	6.42	7.02									
	2.4	1.5									
H δ $\lambda 4102$											
	0.23	0.19	0.18	0.17		0.20	0.17	0.28			
	0.26	0.26	0.26	0.26		0.28	0.26	0.37			
	12.46	11.37	2.97	3.41		3.63	2.57	3.81			
	6.3	3.0	3.0	2.3		2.7	4.3	1.8			
[O III] $\lambda 4959$											
	0.28	0.51	0.37	0.17	0.23	0.22	0.27	0.12	0.49	0.29	
	0.27	0.48	0.32	0.15	0.20	0.20	0.23	0.11	0.42	0.23	
	17.93	27.68	5.13	3.19	2.90	4.49	3.27	1.41	8.36	2.15	
	7.2	9.4	5.6	3.3	3.0	4.3	5.9	1.8	3.3	2.8	
[O III] $\lambda 5007$											
	0.80	1.56	1.05	0.48	0.69	0.65	0.89	0.37	1.48	0.70	0.85
	0.78	1.46	0.91	0.44	0.60	0.59	0.77	0.32	1.26	0.56	0.84
	51.61	86.77	14.42	9.73	8.59	13.00	11.07	4.23	25.12	5.11	34.99
	24.3	25.4	18.9	8.0	8.9	10.0	15.3	3.6	10.4	6.1	4.7

Table 3 continued

	R1	R2	R3	R4	R5	R6	R7	R8a	R8b	R8c	R9
[O I] λ 6300	0.05										
	0.05										
	4.10										
	1.4										
[N II] λ 6548	0.33	0.27	0.39	0.44	0.47	0.47	0.31	0.48	0.66	0.52	
	0.32	0.21	0.34	0.39	0.38	0.43	0.27	0.41	0.45	0.41	
	29.74	17.91	7.53	11.14	7.00	15.61	4.12	9.86	12.15	13.77	
	12.1	6.4	7.6	6.1	5.4	7.4	6.3	2.8	5.3	4.0	
H α λ 6563	2.87	2.86	3.13	3.14	3.70	3.40	2.67	3.45	4.20	3.27	2.24
	2.76	2.17	2.81	2.86	3.08	3.14	2.45	3.04	2.94	2.78	2.22
	252.4	187.4	61.49	80.39	56.18	113.70	35.08	71.32	77.23	33.09	447.10
	58.5	41.6	47.5	38.8	27.8	39.9	37.9	21.7	22.3	22.2	11.1
[N II] λ 6583	0.95	0.83	1.23	1.33	1.48	1.43	0.90	1.23	1.66	1.36	1.09
	0.91	0.62	1.07	1.18	1.19	1.30	0.78	1.05	1.13	1.09	1.08
	80.96	54.39	24.21	34.39	22.95	48.56	11.83	25.39	30.44	13.77	217.70
	26.7	18.2	23.2	20.6	18.6	22.6	23.4	11.2	11.4	11.1	5.9
He I λ 6678		0.03									
		0.02									
		1.90									
		1.4									
[S II] λ 6717	0.28	0.22	0.49	0.57	0.74	0.53	0.25	0.66	0.63	0.76	
	0.27	0.16	0.43	0.51	0.59	0.48	0.22	0.56	0.42	0.61	
	26.37	15.55	9.66	15.38	11.96	17.62	3.41	11.65	9.92	7.45	
	7.7	6.5	8.3	7.7	8.1	8.4	6.9	5.8	5.3	5.6	

Table 3 continued

	R1	R2	R3	R4	R5	R6	R7	R8a	R8b	R8c	R9
[S II] $\lambda 6731$	0.20	0.13	0.33	0.38	0.53	0.38	0.21	0.46	0.36	0.49	
	0.19	0.09	0.29	0.34	0.42	0.34	0.18	0.39	0.24	0.39	
	17.53	8.98	6.44	10.03	8.56	12.63	2.75	8.15	5.66	4.74	
	5.4	2.7	5.9	5.2	6.1	7.2	4.8	4.0	3.7	4.1	
H β $\lambda 4861$											
$f_{H\beta}$	5.98	3.63	4.78	2.10	1.86	4.51	2.94	0.97	0.97	1.21	0.88
$I_{H\beta}$	6.59	8.64	5.50	2.51	2.82	4.96	3.39	1.14	2.52	1.51	0.89
	68.76	54.02	13.34	22.75	13.58	19.80	13.27	12.01	14.38	8.12	147.30
	25.6	16.9	17.6	12.6	10.5	13.2	17.6	7.3	6.9	5.8	6.1

1: The ratio of the uncorrected line flux to that of H β . For H β the flux is given in units of 10^{-16} erg s $^{-1}$ cm $^{-2}$ Å $^{-1}$.

2: The ratio of the reddening corrected line flux to that of H β . For H β the flux is given in units of 10^{-16} erg s $^{-1}$ cm $^{-2}$ Å $^{-1}$.

3: The measured equivalent width in Ångstroms of the line (no absorption correction has been applied to the values for the Balmer lines).

4: The statistical signal to noise of the line.

Table 4 – Derived Results

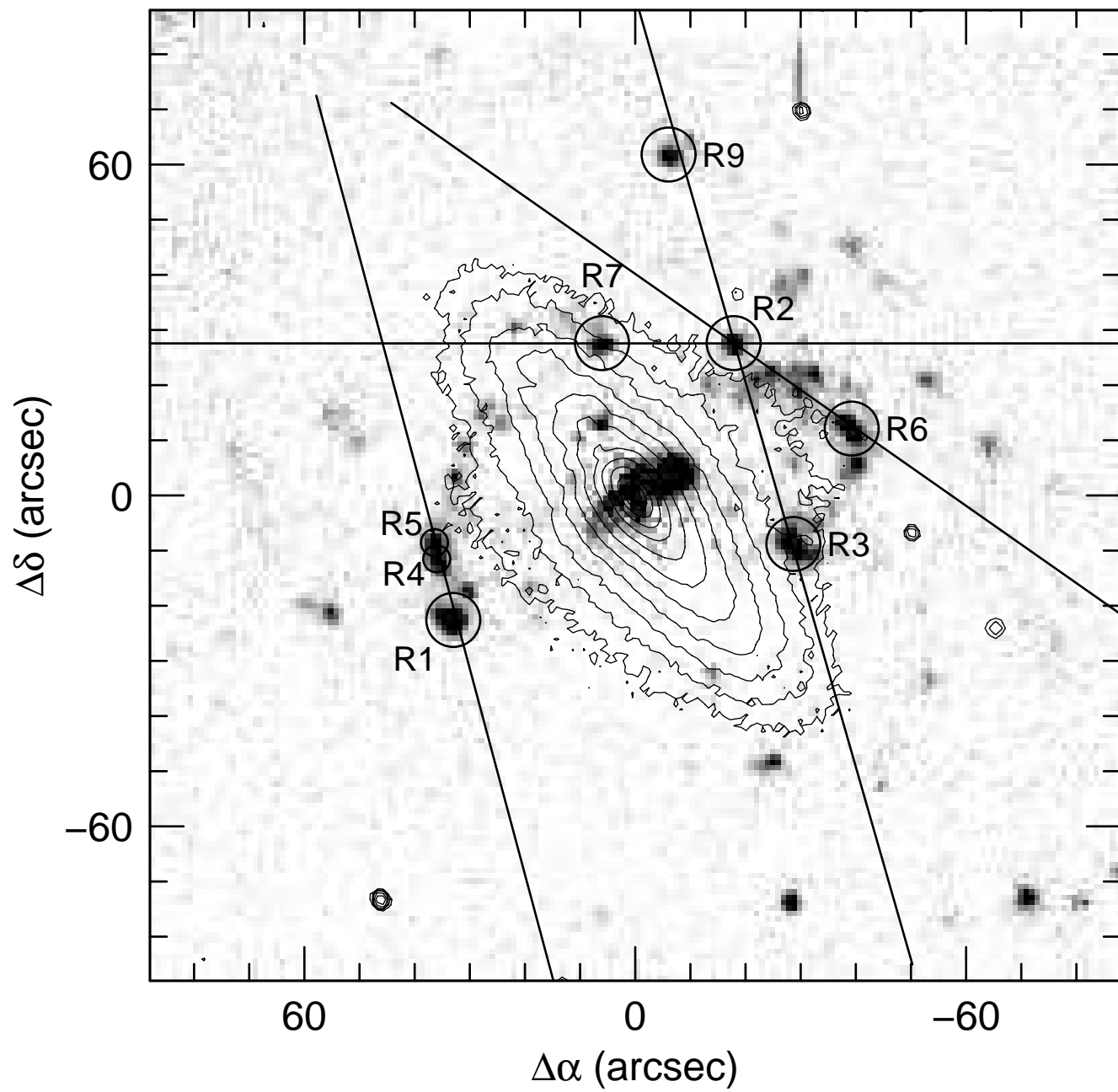
H II Region	Offset ¹ "E,"N	T_e K	N_e cm ⁻³	A_V mag.	R_{23}	12+log(O/H)	Range ²
R1	33, -22	<11500	41	0.06	2.67	8.94	8.93–8.95
R2	-19, 28	< 8700	<10	0.77	4.08	8.83	8.81–8.86
R3	-29, -8	<11800	<10	0	3.02	8.92	8.90–8.93
R4	35, -12	<15500	<10	0.08	2.80	8.94	8.91–8.96
R5	36, -8	<18900	41	0.26	2.61	8.95	8.92–8.98
R6	-40, 13	<13300	57	0	2.57	8.95	8.93–8.97
R7	5, 28	<12700	232	0	2.67	8.94	8.92–8.96
R8a	-30, 20	<29100	25	0	2.22	8.98	8.93–9.00
R8b	-25, 23	<15600	<10	0.77	4.15	8.82	8.77–8.90
R8c	-23, 21	<20000	<10	0	2.76	8.94	8.88–8.98
R9	-7, 62			0	<3.03	>8.92	8.84–8.97

1. With respect to the central position, given in Table 1.

2. The 1σ statistical range in 12+log(O/H) derived from the counting statistics of the line fluxes.

Fig. 1.— NGC 2685 in H α (greyscale) and red continuum (contours). The H α emission shows the H II regions in the inner and outer rings, as well as the central LINER emission region. The line-segments show the placement of the spectrograph slit. The labelled circles show the H II regions observed. For clarity, the three observed components of the H II complex R8 are not labelled. They lie between R2 and R6.

Fig. 2.— Fully reduced, flux calibrated spectra of two H II regions in NGC 2685, showing the full range in signal to noise of our spectra. The spectra shown are from a) R2 with 7 hours total integration, and b) R9 with 2.5 hours total integration. The spectral features identified in R2 are labelled in a).



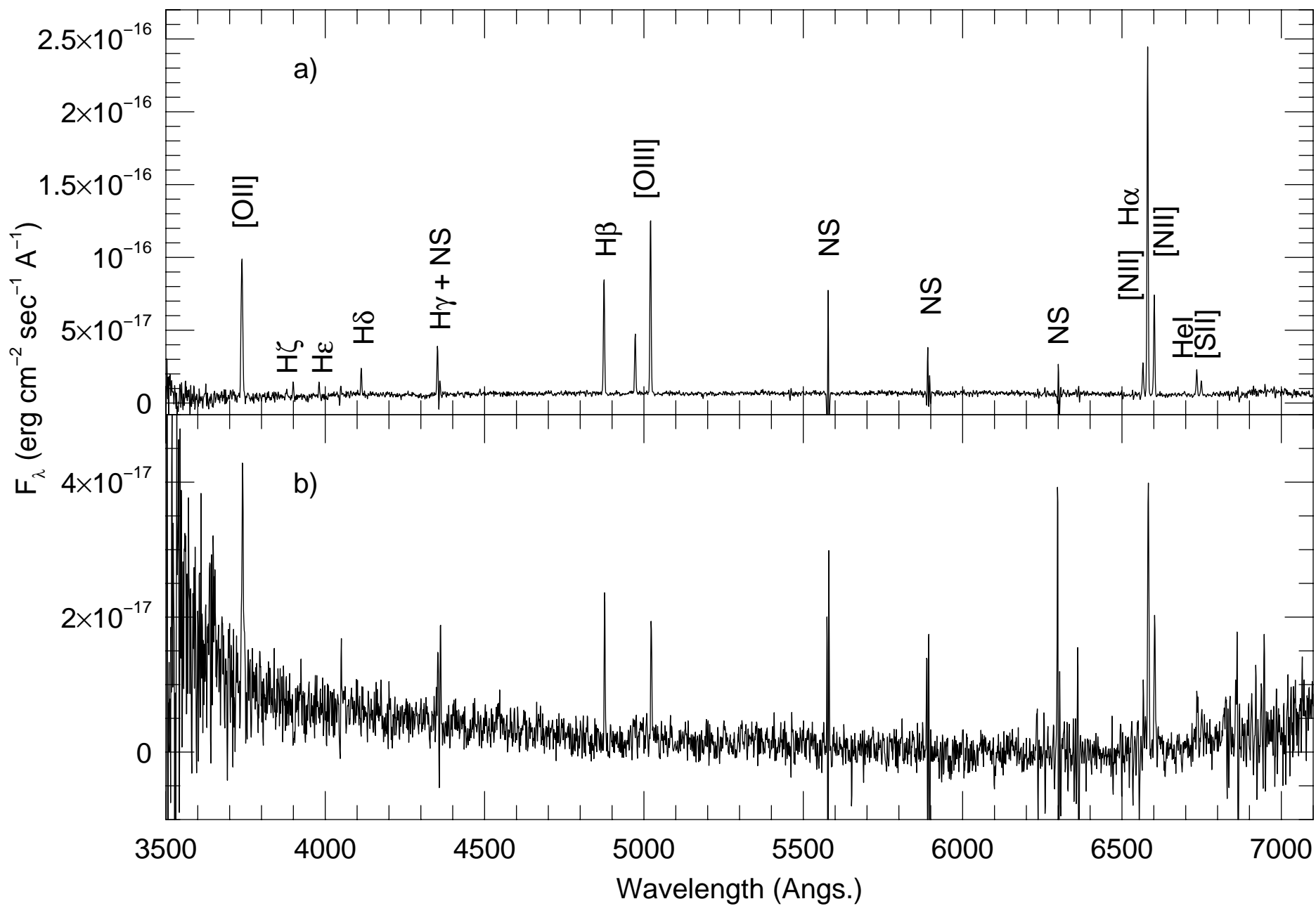


Figure 2